Journal of Materials Chemistry A

Phosphonium zwitterions for lighter and chemically-robust MOFs: Highly reversible H2S capture and solvent-triggered release

Journal:	*Journal of Materials Chemistry A*
Manuscript ID	TA-ART-05-2019-005444
Article Type:	Paper
Date Submitted by the Author:	22-May-2019
Complete List of Authors:	Reynolds III, Joseph; The University of Texas at Austin, Chemistry & Biochemistry Bohnsack, Alisha; The University of Texas at Austin, Chemistry & Biochemistry Kristek, David; The University of Texas at Austin, Chemistry & Biochemistry Gutierrez-Alejandre, Aida; Universidad Nacional Autónoma de México, Facultad de Química, Ingeniería Química Dunning, Samuel; The University of Texas at Austin, Chemistry & Biochemistry Waggoner, Nolan ; University of Texas at Austin, Chemistry Sikma, Ronald; The University of Texas at Austin, Chemistry & Biochemistry Ibarra, Ilich; Universidad Nacional Autónoma de México, Instituto de Investigaciones en Materiales Humphrey, Simon; The University of Texas at Austin, Chemistry & Biochemistry

Journal Name

EDGE ARTICLE

Phosphonium zwitterions for lighter and chemically-robust MOFs: Highly reversible H_2S capture and solvent-triggered release

Joseph E. Reynolds III,[a] Alisha M. Bohnsack,[a] David J. Kristek,[a] Aída Gutiérrez-Alejandre,[b] Samuel G. Dunning,[a] Nolan W. Waggoner,[a] R. Eric Sikma,[a] Ilich A. Ibarra[c,]* and Simon M. Humphrey[a,]*†

Received 00th January 20xx,
Accepted 00th January 20xx

DOI: 10.1039/x0xx00000x

www.rsc.org/

The tetrahedral zwitterion of *tetrakis*(*p*-carboxyphenyl) phosphonium is structurally analogous to a family of ligands with C or Si cores that have found great utility in the preparation of stable MOFs. However, the central P(V)$^+$ core in this molecule reduces the formal ligand charge, resulting in a PR_4^{3-} *tetra*(carboxylate) species. This new strategy allows for the formation of lighter MOFs by incorporation of less metal, which cannot be accessed using conventional ligands. The phosphonium zwitterion is stable under hydrothermal synthesis conditions; it spontaneously crystallizes from hot DMF to give a metal-free and infinitely porous ionic hydrogen-bonded organic framework, which is stable in water and organic solvents. We demonstrate how direct hydrothermal treatment of the ionic framework in the presence of $In(NO_3)_3$ yields a new charge-neutral In(III) MOF with diamondoid topology. By comparison, solvothermal reaction in the presence of $Mg(NO_3)_2$ yields a chemically-robust MOF with permanent 3D porosity. The Mg(II)-based MOF displays water adsorption properties with an estimated ΔH_{ads} of –63.5 kJ mol^{-1} and a maximum uptake of 38.9 wt% at 30 °C. This exceptionally stable material also showed highly reversible H_2S sorption with a capacity of ~8 mmol g^{-1}, and solvent-triggered H_2S release.

Introduction

The rational design of metal-organic frameworks (MOFs) with desired net types has become an established art. Control over network connectivity through precise combinations of organic and inorganic building blocks with complimentary geometric elements has been summarized eloquently in recent review articles.[1] Conventionally, MOFs are comprised of anionic ligands, L^{n-}, coordinated to cationic metal ions or clusters, M^{m+}; charge-balance is achieved based on the formation of materials with suitable M:L ratios. Although MOFs with net anionic or cationic frameworks and pore-based counterions are known,[2] charge-neutral MOFs are by far the most common, since solution-phase MOF synthesis in the presence of excess H^+ or OH^- provides numerous possibilities under which charge-neutral products are obtained. In general, MOFs prepared with highly charged metal and ligand species are found to be both chemically and thermally more stable (*e.g.*, UiO-66 based on Zr(IV) nodes[3]), while MOFs based on low-valent metals and neutral ligands (*e.g.*, Cu(I) cyanide polymers[4]) are much less stable. However, MOFs that incorporate heavy metals and/or larger multi-metal clusters as their nodes are correspondingly more dense, thus resulting in lower overall gravimetric sorption capacities.

From the perspective of the types of organic ligands commonly used in MOF synthesis (*i.e.* carboxylates,[1b,c] imidazolates,[5] *etc.*), it is clearly a much greater challenge to reduce the anionic charge, without physically removing one or more anionic donor substituents. However, ligands with multiple anionic substituents are required to form MOFs with 3D connectivity that support stable micropore networks. For example, there are three possible structural isomers of benzene tricarboxylic acid (btc; 1,2,3- 1,2,4- and 1,3,5-). When employed as MOF building blocks, these ligands result in completely different network types by reaction with the same metal ions.[6,7] For example, HKUST-1 (Cu_3(1,3,5-btc)$_2$ is obtained using the C_3-symmetric trimesate isomer,[7] while the lower-symmetry 1,2,3- and 1,2,4- isomers lead to MOFs with correspondingly lower network symmetries.[6a,d] Yet all three fully deprotonated btc ligands carry the same 3– charge, requiring the same proportion of metal ions (M^{m+}) to achieve overall framework charge-balance. This example underlines how ligand geometry provides control over framework topology, while the exercising synthetic control over the M:L ratio is significantly more difficult to achieve.

[a] Department of Chemistry, The University of Texas at Austin, Welch Hall 2.204, 105 E. 24th St. Stop A5300, Austin TX 78712-1224 U.S.A. Email: smh@cm.utexas.edu.
[b] Unidad de Investigación en Catálisis, Depto. de Ingeniería Química, Facultad de Química, Universidad Nacional Autónoma de México, Circuito Exterior s/n, CU, Del. Coyoacán, 04510, Ciudad de México, Mexico. Email: argel@unam.mx
[c] Laboratorio de Fisicoquímica y Reactividad de Superficies (LaFReS), Instituto de Investigaciones en Materiales, Universidad Nacional Autónoma de México, Circuito Exterior s/n, CU, Del. Coyoacán, 04510, Ciudad de México, Mexico.

† Electronic Supplementary Information (ESI) available: Additional experimental details, characterizing data and spectroscopic data for the compounds. See DOI: 10.1039/x0xx00000x. CCDC numbers 1904837-1904839 contain the CIF data for iPCM-1, PCM-66 and PCM-75, respectively.

These design considerations led us to consider the following question: *how can we prepare stable MOFs using established and highly-connected* poly*(carboxylate) ligands, while simultaneously formally reducing the ligand anionic charge (L^{n-}) to permit the formation of lower-density materials?*

We chose to address this question *via* the incorporation of heavier (3*p* & 4*p*) atoms into ligands of pre-existing interest to MOF chemists, in which the expanded valencies and variable oxidation states available to these elements can be exploited to modify the ligand charge. As part of our ongoing studies into the formation of MOFs based on arylphosphines (the so-called phosphine coordination materials, or PCMs), we showed that methylation of *tris*(4-carboxyphenyl)phosphine, $P(C_6H_4\text{-}4\text{-}CO_2H)_3$, with methyl iodide was a simple but powerful way to lower the overall charge of the triply deprotonated ligand to give a net *dianionic* species, $[P(CH_3)(C_6H_4\text{-}4\text{-}CO_2)_3]^{2-}$.[8] Importantly, this strategy does not alter the geometrical nature of the ligand as a tritopic MOF building block. However, the phosphonium derivative did provide access to lighter, charge-neutral frameworks based on 1:1 M^{2+}:L^{2-} ratios (*versus* a 3:2 M^{2+}:L^{3-} ratio dictated by the parent phosphine) by incorporation of proportionately mess total metal.[8a,b]

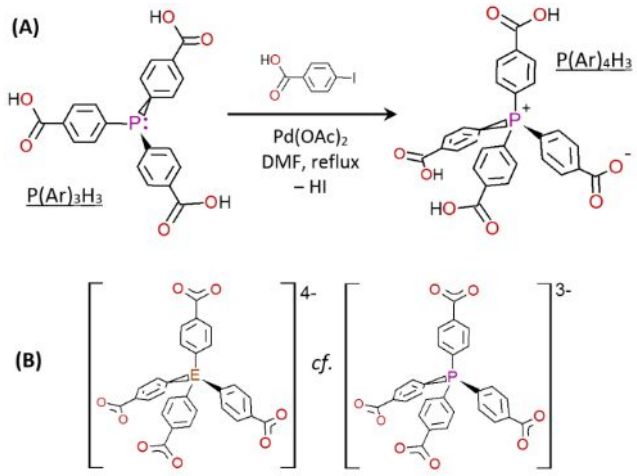

Scheme 1. (A) Synthetic route to obtain the tetrahedral phosphonium zwitterion, $P(Ar)_4H_3$; **(B)** structure and charge comparison of known tetracarboxylate building blocks (where E = C, Si, 1,3,5,7-adamantyl, *etc*.) *versus* the phosphonium tetracarboxylate trianion.

Results and Discussion

In the present work we have extended this approach to prepare a more highly symmetric tetrahedral, tetratopic phosphonium species ($P(Ar)_4H_3$; Scheme 1A). The target phosphonium was obtained in high yield by Pd(II)-catalysed P–C coupling of 4-iodobenzoic acid with the parent phosphine in refluxing *N*,*N*-dimethylformamide (DMF; Scheme 1A). We targeted this ligand because several structurally analogous ligands based on C,[9] Si[10,9d] and other larger tetrahedral cores (*e.g.*, 1,3,5,7-adamantyl)[9c,d,11] have already been explored widely in MOF synthesis by Yaghi and others, using a reticular approach.[9c-d, 10a] The tetrahedral geometry of this ligand class leads to robust 4,4-connected diamondoid MOFs in combination with tetrahedral metal ions or clusters.[9-11] The critical difference between the fully deprotonated versions of these ligands and our P(V)-based phosphonium analogue is shown in Scheme 1B: both ligands are geometrically equivalent tetratopic linkers; but the latter is formally *trianionic* due to the charge carried by the central $P(V)^+$ atom.

Organophosphonium salts are widely employed in materials synthesis because the enhanced thermal and chemical stability of the P^+–C bonds renders them suitable for reactions at higher temperatures, and in aqueous media. Phosphonium salts are also increasingly important as robust ionic liquids.[12] Yet, to the best of our knowledge, there are no previous examples of tetrahedral phosphonium-based MOFs.

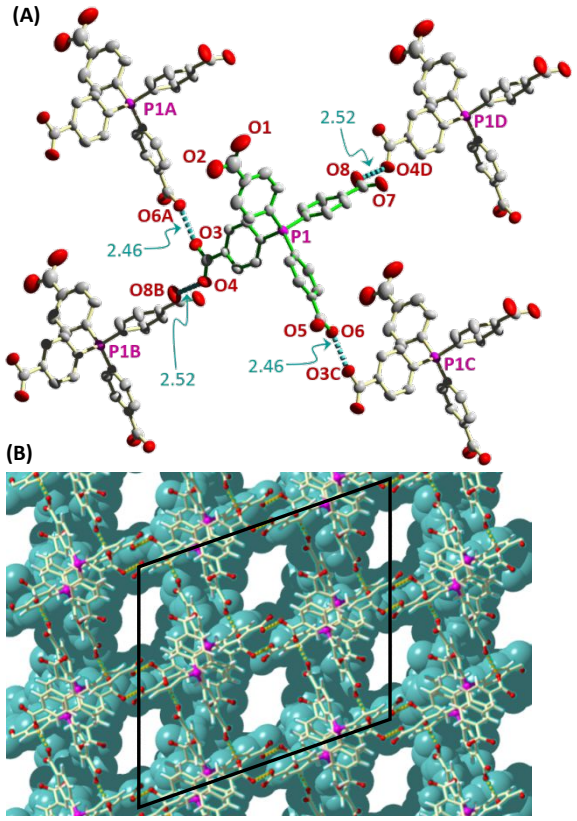

Figure 1. (A) Crystal structure of iPCM-1 showing H-bonding environment (cyan dashed bonds and distances in Å) around each unique $P(Ar)_4H_3$ zwitterion; thermal ellipsoids are drawn at the 50% probability level and H-atoms are omitted for clarity. **(B)** Space-filling rendering of the resulting 4,4-connected network and open pore structure in iPCM-1 when viewed in the crystallographic *ac*-plane.

Our initial expectation was to isolate the target phosphonium ligand precursor as an iodide adduct $[P(C_6H_4\text{-}4\text{-}CO_2H)_4]^+ I^-$, in a similar fashion to our previous synthesis of $[P(CH_3)(C_6H_4\text{-}4\text{-}CO_2H)_3]^+ I^-$.[8a] Surprisingly, however, large colourless crystals of the product formed directly from the DMF mother liquor upon cooling of the P–C coupling reaction (Scheme 1A). Single crystal X-ray diffraction (SCXRD) analysis revealed that the target phosphonium had been successfully obtained, but each molecule was singly deprotonated as a charge-neutral $\{P^+(C_6H_4\text{-}4\text{-}CO_2H)_3(C_6H_4\text{-}4\text{-}CO_2^-)\}$ zwitterion, accompanied by the loss of one equivalent of HI. The result was a 3D-connected microporous hydrogen-bonded organic framework (*i.e.*, HOF[13]), in which delocalized H^+ ions act as 'ultra-light metal' cations (Figure 1A).

The structure of the zwitterionic solid, hereby referred to as iPCM-1 (ionic Phosphine Coordination Material) was solved in the monoclinic space group $I2/a$ (Z = 8) with formula, $[H_3\{P(C_6H_4\text{-}4\text{-}CO_2)_4\}\cdot 2DMF\cdot \frac{1}{2}H_2O]_\infty$. The asymmetric unit contains one complete crystallographically-unique phosphonium molecule; the central P(V) atom is *pseudo*-tetrahedral with C–P–C bond angles ranging between 105.8(3)–113.4(3)° (P1; Figure 1A). All four *para*-carboxylate moieties are approximately co-planar with respect to their parent aromatic rings. Elemental microanalysis and thermogravimetric analysis (TGA) of bulk iPCM-1 samples agreed with the SCXRD solution, to confirm that no halide was present in the lattice (see ESI). Therefore, each phosphonium monomer is associated with 3 carboxylate-H atoms. A closer inspection of the crystal structure reveals a single full-occupancy DMF solvate molecule, which is coordinated in a classical H-bonded dimer orientation with the carboxylate group labelled as O1 and O2 (Figure 1A); the O2···O^{DMF} distance is 2.76 Å, indicative of a moderately strong H-bonding interaction.[14] This also infers that O2 is fully protonated, leaving two H^+ ions to be shared between the remaining three carboxylates. There are two very short intermolecular carboxylate contacts that bridge between three adjacent phosphonium molecules, with O···O distances of 2.46 and 2.52 Å (O3···O6A and O4···O8B, respectively; Figure 1A). According to Jeffrey, these distances constitute strong hydrogen bonding interactions.[14] As shown by the blue dashed bonds in Figure 1A, one carboxylate is *syn*,*anti*-bridged while the other two are monodentate.

The overall result is an undulating, 3D network of ionic hydrogen bonded molecules, which support small micropores (Figure 1B). The micropores are filled with additional partial-occupancy DMF and H_2O solvate molecules. The micropore network in iPCM-1 consists of 1D channels that lie parallel to the crystallographic *b*-axis and have rhombic shaped windows with a maximum accessible opening of 7.2 Å (Figure 1B).

Comparison of the bulk powder X-ray diffraction (PXRD) pattern with the pattern simulated from the single crystal data confirmed the phase purity of iPCM-1 (Figure 2A). In support of the TGA findings (Figure S13), iPCM-1 retained its crystallinity upon evacuation at 150 °C, but the PXRD pattern observed was markedly different to that of the as-synthesised material (Figure 2A; yellow data), indicative of a phase transition to a smaller unit cell. The desolvated powder pattern was also similar to that obtained by subjecting as-synthesized iPCM-1 to cycles of solvent exchange using acetone. When fresh samples were immersed in H_2O, the DMF solvates were exchanged and the material exhibited a phase change to a new crystalline structure, (Figure 2A; purple data). Solvent exchange with tetrahydrofuran (THF) gave a PXRD pattern that was intermediate between the original and desolvated structure (Figure 2A; blue data).

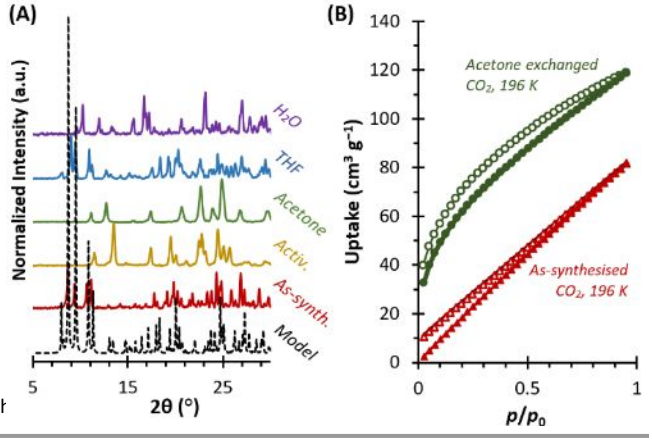

Figure 2. **(A)** Comparison of PXRD data for iPCM-1 upon desolvation and re-immersion in different solvents. **(B)** CO_2 sorption isotherms for iPCM-1 based on activation conditions, showing lack of saturation at 1 atm; closed symbols = adsorption, open symbols = desorption.

All of the above indicate that iPCM-1 shows not only broad solvent stability, but also 'soft crystalline' behaviour.[15] iPCM-1 was not dissolved upon standing in a range of organic solvents (chloroform, dichlorom ethane, methanol, ethanol, isopropanol, acetonitrile, 1,4-dioxane, *N*-methylpyrrolidone, pyridine, ethyl acetate, diethyl ether, hexanes) and was only eventually solubilised in strongly basic water (pH > 9). This is rather unusual in comparison to typical crystallized organic molecules, which tend to undergo dissolution or lose crystallinity under these conditions, and is likely due to the highly ionic structure and strong hydrogen bonding network in iPCM-1.

Desolvated samples of as-synthesized iPCM-1 displayed low affinity for N_2 gas at 77 K (Figure S14), but an appreciable BET surface area of 191 $m^2\,g^{-1}$ was obtained using CO_2 at 196 K, corresponding to a capacity of 81.6 $cm^3\,g^{-1}$ at 1 atm (Figure 2B; red triangles). Acetone exchange led to a significant enhancement of the CO_2 surface area, yielding 273 $m^2\,g^{-1}$ (107.8 $cm^3\,g^{-1}$ at 196 K; Figure 2B; green circles). The CO_2 isotherms did not reach saturation at 1 atm, as has been observed for other microporous materials including HOFs.[8b-d]

Although the serendipitous formation of the porous organic crystalline iPCM-1 led to an interesting new material, we continued to pursue the preparation of new MOFs using iPCM-1 itself as a precursor. First, the stability of the phosphonium zwitterion was assessed by heating iPCM-1 to 200 °C in water for sustained periods using Teflon-lined autoclaves. Upon cooling, the ligand was recovered as a microcrystalline solid; SCXRD analysis revealed that the phosphonium species was intact, and was found to recrystallise into a number of different non-porous polymorphs. In stark contrast, the parent phosphine ligand ($P(Ar)_3H_3$; Scheme 1A) undergoes hydrolysis under hydrothermal conditions at temperatures above *ca.* 100 °C to yield phosphinic acid ($R_2P(=O)OH$; accompanied by loss of benzoic acid). At increasingly elevated temperatures, complete hydrolysis leads to the formation of PO_4^{3-}.

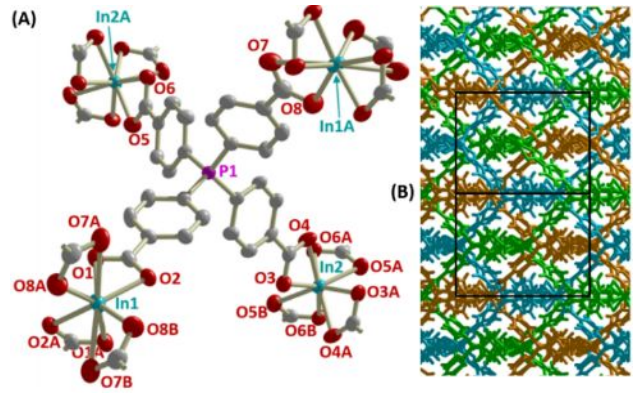

Figure 3. **(A)** Extended asymmetric unit of In(III)-based PCM-66 showing tetrahedral 4,4-connectivity. **(B)** Triple interpenetration when viewed in the crystallographic *bc*-bisector.

Next, iPCM-1 (or alternative polymorphs of the zwitterion) was treated with various metal precursors under hydrothermal conditions. To begin with, we employed various M^{3+} precursors that are known to support tetrahedral coordination environments (including $Al(NO_3)_3$, $Cr(acac)_3$, $Cr(NO_3)_3$, $Cr_2(SO_4)_3$, $FeCl_3$, $Fe(NO_3)_3$, $InCl_3$, $In(NO_3)_3$) with the aim of preparing diamondoid (4,4-connected) networks based on simple 1:1 M^{3+}:L^{3-} ratios; excess base (KOH) was also systematically added. No isolable products were obtained for any of the lighter aforementioned metals, but reaction of the ligand with $In(NO_3)_3$ in pH neutral water at 160 °C produced colourless prismatic shards suitable for SCXRD, revealing the discovery of a new MOF, referred to as PCM-66. The structure was solved in the tetragonal space group $I\bar{4}$ (Z = 8) with formula $[In\{P(C_6H_4\text{-}4\text{-}CO_2)_4\}]_\infty$ adhering to the targeted 1:1 M^{3+}:L^{3-} ratio (Figure 3). The asymmetric unit of PCM-66 contains two crystallographically unique In(III) atoms located on 2-fold inversion centres, and one complete phosphonium ligand (Figure 3A). Both In(III) centres are 8-coordinate with approximate dodecahedral geometry arising due to coordination by four chelating carboxylates; each isolated In(III) site is therefore a *pseudo*-tetrahedral 4-connected node within the framework of PCM-66. Accordingly, all of the carboxylate substituents *per* ligand are coordinated by In(III), resulting in a highly symmetric 4,4-diamondoid net (Figure 3B). PCM-66 crystalized as a triply interpenetrated structure with three interwoven 4,4-nets, giving a dense solid that did not contain additional solvent of crystallization, supported by elemental microanalysis, TGA and gas sorption data (Figures 3B & ESI). To date, we have been unable to prepare non-interpenetrated versions of PCM-66 and interpenetration is common in 4,4-connected MOFs.[16]

Our next idea was to employ Mg(II) salts to synthesize low-density MOFs based on 3:2 M^{2+}:L^{3-} ratios that compare more favourably than analogous MOFs prepared with conventional tetrahedral ligands, which require a 2:1 M^{2+}:L^{4-} ratio. There is a great deal of current interest in the synthesis of Mg(II)-based MOFs because they exhibit high thermal stability, and Mg is cheap, readily available, and non-toxic.[17] Isolated Mg(II) ions predominantly favour octahedral coordination, but small Mg clusters (*i.e.,* 2–4 Mg ions) have been shown to provide symmetric nodes of higher connectivity in the MOF setting.[17a,c,18] Reaction of 3 eq. of $Mg(NO_3)_2$ with the zwitterion at 85 °C over 15 hours in a DMF/MeOH/H_2O (5:2:1 v/v) mixture produced high-yields of colourless rod-shaped crystals. SCXRD analysis revealed a new 3D MOF, hereby referred to as PCM-75. The structure was solved in the orthorhombic space group, $Ibca$ (Z = 8). The framework is net neutral with repeat unit, $[Mg_3\{P(C_6H_4\text{-}4\text{-}CO_2)_4\}_2(OH_2)_2]_\infty$ in addition to DMF and H_2O solvates.

Figure 4A shows the extended asymmetric unit of PCM-75, which includes a single unique phosphonium ligand that is multiply

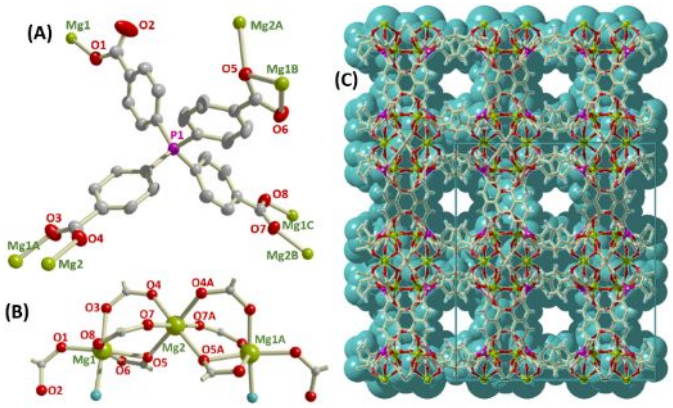

Figure 4. **(A)** Extended asymmetric unit of Mg(II)-based PCM-75 showing the ligand connectivity. **(B)** Extended metal node showing the connectivity of the Mg(II) trimer. **(C)** Space-filling view down the *b*-axis of PCM-75 displaying the largest pore window present within the framework.

coordinated to two unique Mg(II) ions. The phosphonium adopts a regular tetrahedral geometry with C–P–C bond angles between 106.4–112.3°. Seven of the eight carboxylate-*O* atoms are coordinated, with only O2 uncoordinated. The metal nodes in PCM-75 are $[Mg_3(OCO)_8(OH_2)_2]^{2-}$ units consisting of *pseudo*-octahedral Mg(II) ions (Figure 4B). Each Mg1 atom is coordinated by five carboxylate-*O* donors and a single terminal OH_2 ligand (blue atom, Figure 4B); Mg2 resides on a crystallographic inversion centre and is triply bridged to each neighbouring Mg1 atom. Overall, each Mg_3 cluster is an 8-connected framework node, resulting in a non-interpenetrated material with 8,4-connectivity.

In comparison to the interpenetrated In(III)-based PCM-66, the metal atom labelled Mg2 in PCM-75 can be considered as acting to fuse two adjacent 4,4-connected diamondoid nets to provide a single, open framework (Figure 4B & C). PCM-75 supports inter-connected micropore openings in all three crystallographic directions (Figure 4C & S20). The largest pores lie along the crystallographic *b*-axis with a guest-accessible opening of 6.8 Å^2 (Figure 4C). A comparison of the TGA profiles of as-synthesized PCM-75 *versus* a sample pre-activated under vacuum at 250 °C to remove all pore-based solvent molecules reveals an approximate 11.5% mass loss due to weakly adsorbed solvent. Under these conditions, elemental analysis confirmed that all DMF had been removed (ESI). The as-synthesized material shows a gradual and continuous mass loss from 25 to 485 °C. Regardless of the activation conditions, the onset of framework decomposition in PCM-75 did not occur until *ca.* 485 °C, which is similar to what has been observed for other Mg(II)-based MOFs (Figure S21). An interesting observation arising from the TGA studies concerned the apparent affinity of desolvated PCM-75 to rapidly re-adsorb atmospheric H_2O. Even upon rapid transfer of desolvated PCM-75 to the TGA apparatus, the material appeared to have adsorbed 8 H_2O molecules *per* formula unit. This finding was confirmed by elemental analysis of a PCM-75 sample activated at 250 °C and then re-exposed to the air (ESI).

The bulk PXRD pattern of as-synthesized PCM-75 was well-matched with the theoretical pattern simulated from the SCXRD solution. Upon desolvation at 250 °C in vacuum, the material appeared to have become completely amorphous. But, upon re-exposure to the solvent mixture, the original crystallinity was completely recovered (Figure S22). Equally, the structure of PCM-75 was recovered upon exposure to other common organic solvents.

Next, to assess the bulk porosity of PCM-75 and its optimum activation conditions, as-synthesized samples were heated under vacuum at 75, 150, 200, and 250 °C and then studied by volumetric analysis. Activation at 200 °C yielded the highest surface area and volumetric capacity for N_2, O_2, and H_2 at 77 K as well as for CO_2 and CH_4 at 196 K (Figure 5A & Figures S23-27, Table S1). The BET-derived surface areas obtained using N_2 and CO_2 were, 661 and 800 $m^2\ g^{-1}$, respectively, with corresponding micropore volumes of 0.37 and 0.44 $cm^3\ g^{-1}$. PCM-75 also showed appreciable uptake of O_2, H_2 and CH_4 (290, 171, 122.0 $cm^3\ g^{-1}$); all gases showed highly reversible Type-I adsorption-desorption behaviour (Figure 5A).

Given the hygroscopic nature of PCM-75, we next investigated the water adsorption-desorption properties. The sorption behaviour of as-synthesised PCM-75 activated at 200 °C under flowing N_2 was collected between 0–95% P/P_0 at 30 °C (equivalent to the relative humidity, %RH). Due to the apparent fast sorption kinetics of H_2O in PCM-75, collection of the water adsorption isotherm required a 2 h stabilisation time at each partial pressure point (Figure 5B & ESI). The H_2O adsorption isotherm exhibits a shape indicative of Type-IV adsorption behaviour, in which the water uptake increases gradually from 0 to 40% P/P_0, followed by a more rapid uptake between 40 and

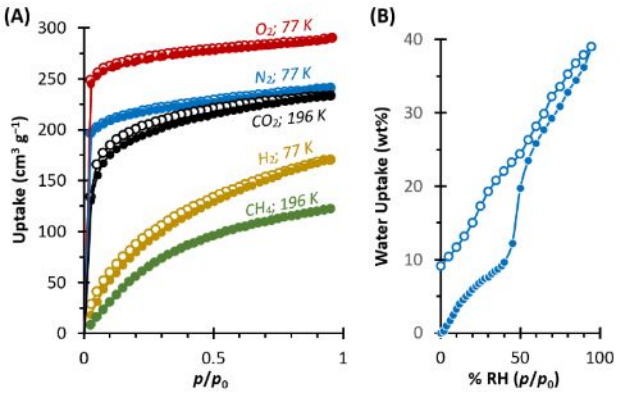

Figure 5. **(A)** Sorption isotherms for PCM-75. **(B)** Water adsorption-desorption isotherm at 30 °C of PCM-75 for %RH = 0–95. Closed circles = adsorption, open circles = desorption.

55% P/P_0; above 55% P/P_0 the uptake increased steadily, reaching a maximum uptake of 38.9 wt% H_2O at 95% P/P_0 (21.6 mmol g^{-1}). The measured H_2O adsorption at intermediate RH (25–45%; most ideal for low-cost atmospheric water capture) is among the best reported so far for MOFs.[19]

The desorption phase showed more linear desorption kinetics over the entire RH range from 95 to 0%, resulting in a marked hysteresis that is most pronounced from 55 to 0% RH, (Figure 5B, open circles). Since the accessible pore openings of PCM-75 (6.7 Å) are considerably larger than the kinetic diameter of H_2O (2.7 Å), the observed hysteresis is unlikely to be due to kinetic trapping behaviour (*i.e.*, bottlenecks within the pores).[20] Instead, the observed hysteresis is most likely due to moderately strong host-guest interactions that causes the desorption process to become more endothermic. H_2O physisorption inside the micropores of PCM-75 may be enhanced due to the polarized nature of the framework, owing to the charged phosphonium species, as well as the presence of highly polarising Mg_3 nodes. In order to quantify this assertion, the isosteric heat of adsorption of H_2O (enthalpy, ΔH_{ads}) was calculated by fitting isotherms recorded at 20 and 30 °C to the Clausius–Clapeyron equation (Figures S28 & S29). This gave an estimated ΔH_{ads} = –63.5 kJ mol^{-1}, which is higher than typical H_2O adsorption enthalpies measured in MOFs (*ca.* –40 to –50 kJ mol^{-1}).[21] Motivated by the interesting H_2O sorption results on PCM-75, we decided to investigate the adsorption properties of hydrogen sulfide (H_2S). H_2S is a colourless gas that is highly corrosive, flammable and toxic to humans.[22] Materials that can reversibly capture large amounts of H_2S from air or effluent streams are topical and technologically important. Dynamic H_2S adsorption (*i.e.*, breakthrough) experiments were performed at 30 °C on activated PCM-75 samples using a 15:85 v/v mixture of H_2S in N_2. The measured H_2S uptake was 8.0 mmol g^{-1} (Figure 6; first cycle), which is the amongst the highest H_2S capture values reported for a MOF material at 30 °C and 1 atm. By comparison, well-studied MOFs including MIL-100(Fe),[23] MIL-53(Fe),[24] HKUST-1,[23] MOF-5,[23] MIL-53(Cr),[24b] Ga-soc-MOF[25] and MIL-125(Ti)[26] showed H_2S capacities of approximately only 1 mmol g^{-1}; in these cases, exposure of the MOF to acidic H_2S gas commonly promoted decomposition of the host

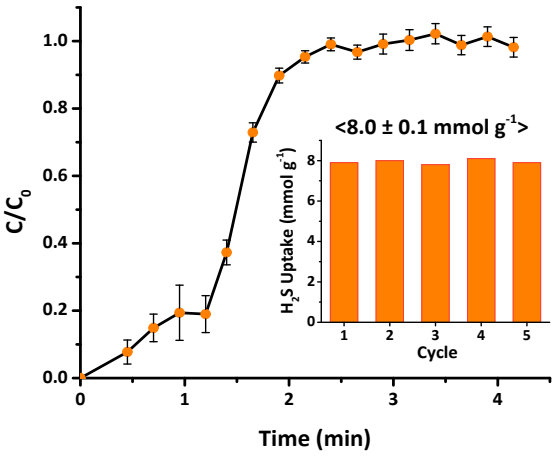

Figure 6. Breakthrough curves of H_2S adsorption by PCM-75 obtained at 30°C and 1 atm using an H_2S feedgas concentration of 15 vol%. The total H_2S/N_2 flow rate was 30 $cm^3\ min^{-1}$. Inset: the comparative adsorption capacities for cycling of the same sample.

material. Notably, another Mg(II)-based MOF (Mg-CUK-1) recently showed highly reversible H_2S capture, with a total capacity of 3.2 mmol g^{-1}.[27] Only CPO-27 (12.0 mmol g^{-1})[28a] and MIL-53(Al)-TDC (18.1 mmol g^{-1})[28b] have achieved higher H_2S sorption capacities.[28]

In order to investigate the recyclability of PCM-75 for H_2S trapping and release, a second H_2S adsorption experiment was conducted on a sample that had been loaded with H_2S and then re-activated under the original activation conditions (12 h, 200 °C, flowing N_2). The total H_2S measured uptake at 1 atm was only 3.1 mmol g^{-1}, less than half of the original capacity. PXRD analysis of re-activated PCM-75 after the initial H_2S loading indicated complete loss of bulk crystallinity

(Figure S30). Elemental analysis of the post-H_2S exposed material upon re-exposure to humid air did not detect S into the MOF, which indicated that H_2S had not been formally incorporated into the MOF scaffold (*e.g.*, by dissociation into H^+ and HS^- as this would be irreversible; see ESI). Together, these results indicated that since the original PCM-75 structure had not been recovered, H_2S gas was apparently physically trapped in the micropores.

Given the soft crystalline behaviour of PCM-75 as already evidenced by PXRD studies (*vide supra*), the H_2S-loaded sample of PCM-75 was immersed in fresh solvent of synthesis (DMF/MeOH/H_2O, 5:2:1 v/v) for 1 h. Subsequent PXRD analysis indicated significant recovery of bulk crystallinity (Figure S30). Time-dependent PXRD studies indicated that no further improvement of crystallinity was obtained upon solvent immersion after 48 h, and in most instances much less time was required to recover the original PCM-75 structure (Figure S30). Furthermore, BET analysis of the sample *post*-immersion gave a CO_2 surface area of 802 $m^2\ g^{-1}$, which

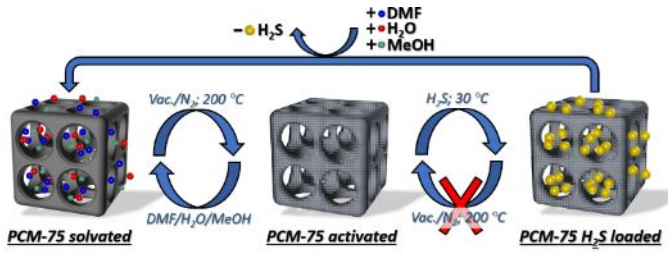

Scheme 2. Proposed mechanism of H_2S capture and release by PCM-75.

is identical (within instrument error) to the as-synthesised material. The sample was placed in the H_2S breakthrough system and an H_2S experiment was carried out as previously described (see above). The H_2S sorption capacity of the same sample was then collected using identical activation conditions as before, yielding an uptake of 7.8 mmol g^{-1}, (Figure 6; Inset). This surprising result confirmed that PCM-75 was able be completely regenerated between H_2S exposures, simply by using solvent to recover the initial bulk structure, and allowing for the full release of trapped H_2S. In fact, this process was conducted a further 3 times, showing comparable H_2S sorption capacities in each case (Figure 6 Inset & Scheme 2).

To the best of our knowledge, this is the first demonstration of highly cyclable and high-capacity H_2S trapping and release by a MOF, in which the release and regeneration step is solvent-triggered (Scheme 2). CPO-27[28a] demonstrated triggered release of H_2S by small molecules, suggesting that the actual mechanism of H_2S release may be very similar.

In an attempt to better understand the flexible nature of PCM-75 upon H_2S loading, an *in situ* PXRD experiment was carried out by exposing an activated PCM-75 sample to 1 atm H_2S/N_2 in a sealed capillary tube (Figure S31). At 30 °C, the sample showed the onset of transition to an amorphous phase after 30 min, and was completely amorphous after 120 min (Figure S31). Immersion of the sample in solvent resulted in full recovery of the original PXRD pattern, with a corresponding CO_2 BET surface area of 783 $m^2\ g^{-1}$.

Conclusions

In conclusion, we have demonstrated the utility of a hydrothermally-stable tetrahedral phosphonium zwitterion $\{P^+(C_6H_4\text{-}4\text{-}CO_2H)_3(C_6H_4\text{-}4\text{-}CO_2^-)\}$ as a new building block for the synthesis of MOFs, whose assembly requires less metal than MOFs based on charge-neutral C/Si-based analogues. In our initial studies, the phosphonium ligand was used in the synthesis of two new, low-density MOFs based on In(III) (PCM-66) and Mg(II) (PCM-75). The latter displayed unusually high chemical stability, allowing for the fully cyclable sorption of H_2S gas, with an impressive H_2S capacity of 8.0 ±0.1 mmol g^{-1}. H_2S release and regeneration of the material was found to be solvent-triggered. PCM-75 also displayed a high affinity for water vapour with a maximum uptake of 38.9 wt% at 30 °C. The zwitterionic nature of the ligand also led to the spontaneous crystallisation of a porous ionic hydrogen-bonded material (iPCM-1), which was structurally stable in both aqueous and organic solvents. This work suggests that this and other related phosphonium ligands will lead to the discovery of other new MOF materials with enhanced structure-function properties.

Conflicts of Interest

The authors declare no conflicts of interest.

Acknowledgements

The authors thank Dr. Vincent M. Lynch (U.T. Austin) for X-ray assistance. T. Jurado-Vázquez (H_2O and H_2S experiments). The authors acknowledge the NSF for funding under grant number DMR-1506694 (S.M.H.), the Welch Foundation (F-1738; S.M.H.), PAPIIT-UNAM (IN101517, I.A.I.) and CONACyT (1789; I.A.I).

Notes and references

1 (*a*) N. Stock and S. Biswas, *Chem. Rev.*, 2012, **112**, 933; (*b*) M. Zhang, M. Bosch, T. Gentle III and H.-C. Zhou, *CrystEngComm.*, 2014, **16**, 4069; (*c*) D. Zhao, D. J. Timmons, D. Yuan and H.-C. Zhou, *Acc. Chem. Res.*, 2011, **44**, 123; (*d*) A. Umemura, S. Diring, S. Furukawa, H. Uehara, T. Tsuruoka and S. Kitagawa, *J. Am. Chem. Soc.*, 2011, **133**, 15506; (*e*) C. Wang, T. Zhang and W. Lin, *Chem. Rev.*, 2012, **112**, 1084; (*f*) T. Islamoglu, S. Goswami, Z. Li, A. J. Howarth, O. K. Farha and J. T. Hupp, *Acc. Chem. Res.*, 2017, **50**, 805; (*g*) W. Lu, Z. Wei, Z.-Y. Gu, T.-F. Liu, J. Park, J. Park, J. Tian, M. Zhang, Q. Zhang, T. Gentle III, M. Bosch and H.-C. Zhou, *Chem. Soc. Rev.*, 2014, **43**, 5561.

2 (*a*) R. Custelcean and B. A. Moyer, *Eur. J. Inorg. Chem.*, 2007, **10**, 1321; (*b*) C. K. Brozek and M. Dinca, *Chem. Soc. Rev.*, 2014, **43**, 5456; (*c*) A. Karmakar, A. V. Desai and S. J. Ghosh, *Coord. Chem. Rev.*, 2016, **307**, 313.

3 (*a*) J. H. Cavka, S. Jakobsen, U. Olsbye, N. Guillou, C. Lamberti, S. Bordiga and K. P. Lillerud, *J. Am. Chem. Soc.*, 2008, **130**, 13850; (*b*) M. Kandiah, M. H. Nilsen, S. Usseglio, S. Jakobsen, U. Olsbye, M. Tilset, C. Larabi, E. A. Quadrelli, F. Bonino and K. P. Lillerud, *Chem. Mater.*, 2010, **22**, 6632.

4 (*a*) B. F. Hoskins and R. Robson, *J. Am. Chem. Soc.*, 1989, **111**, 5962; (*b*) S. R. Batten, A. R. Harris, P. Jensen, K. S. Murray and A. Ziebell, *J. Chem. Soc., Dalton Trans.*, 2000, 3829; (*c*) C.

J. Shorrock, B.-Y. Xue, P. B. Kim, R. J. Batchelor, B. O. Patrick and D. B. Leznoff, *Inorg. Chem.*, 2002, **41**, 6743.

5 K. S. Park, Z. Ni, A. P. Côté, J. Y. Choi, R. Huang, F. J. Uribe-Romo, H. K. Chae, M. O'Keeffe and O. M. Yaghi, *P. Natl. Acad. Sci.*, 2006, **103**, 10186.

6 (*a*) H. A. Habib, J. Sanchiz and C. Janiak, *Dalton Trans.*, 2008, 4877; (*b*) Z. Zhang, J.-F. Ma, Y.-Y. Liu, W.-Q. Kan and J. Yang, *Cryst. Growth Des.*, 2013, **13**, 4338; (*c*) Y. Yan, C.-D. Wu, X. He, Y.-Q. Sun and C.-Z. Lu, *Cryst. Growth Des.*, 2005, **5**, 821; (*d*) C. Ren, L. Hou, B. Liu, G.-P. Yang, Y.-Y. Wang and Q.-Z. Shi, *Dalton Trans.*, 2011, **40**, 793; (e) M. I. H. Mohideen, B. Xiao, P. S. Wheatley, A. C. McKinlay, Y. Li, A. M. Z. Slawin, D. W. Aldous, N. F. Cessford, T. Düren, X. Zhao, R. Gill, K. M. Thomas, J. M. Griffin, S. E. Ashbrook and R. E. Morris, *Nature Chem.*, 2011, **3**, 304.

7 S. S.-Y. Chui, S. M.-F. Lo, J. P. H. Charmant, A. G. Orpen and I. D. Williams, *Science*, 1999, **283**,1148.

8 (*a*) S. M. Humphrey, P. K. Allan, S. E. Oungoulian, M. S. Ironside and E. R. Wise, *Dalton Trans.*, 2009, **13**, 2298; (*b*) P.S. Nugent, V. L. Rhodus, T. Pham, K. Forrest, L. Wojtas, B. Space, M. J. Zarowotko, *J. Am. Chem. Soc.* 2013, **135**, 10950; (*c*) F. Hu, C. Liu, M. Qu, J. Pang, F. Jiang, D. Yuan, M. Hong, *Angew. Chem. Int. Ed.* 2017, **56**, 2101; (*d*) I. A. Ibarra, K. E. Tan, V. M. Lynch and S. M. Humphrey, *Dalton Trans.*, 2012, **41**, 3920; (*e*) N. W. Waggoner, B. Saccoccia, I. A. Ibarra, V. M. Lynch, P. T. Wood and S. M. Humphrey, *Inorg. Chem.*, 2014, **53**, 12674.

9 (*a*) M. Almáši, V. Zeleňák, A. Zukal, J. Kuchára and J. Čejkab, *Dalton Trans.*, 2016, **45**, 1233; (*b*) Y. E. Cheon and M. P. Suh, *Chem. Eur. J.*, 2008, **14**, 3961; (*c*) J. Kim, B. Chen, T. M. Reineke, H. Li, M. Eddaoudi, D. B. Moler, M. O'Keeffe and O. M. Yaghi, *J. Am. Chem. Soc.*, 2001, **123***,* 8239; (*d*) I. Bassanetti; S. Bracco, A. Comotti, M. Negroni, C. Bezuidenhout, S. Canossa, P. P. Mazzeo, L. Marchio and S. P. Luciano, *J. Mater. Chem. A*, 2018, **6**, 14231.

10 (*a*) R. P. Davies, R. Less, P. D. Lickiss, K. Robertson and A. J. P. White, *Cryst. Growth Des*., 2010, **10**, 4571; (*b*) S. Mandic, M. R. Healey, J. M. Gotthardt, K. G. Alley, R. W. Gable, C. Ritchie and C. Boskovic, *Eur. J. Inorg. Chem.*, 2013, 1631-1634; (*c*) C. Liu, F.-Y. Chen, H.-R. Tian, J. Ai, W. Yang, Q.-J. Pan and Z.-M. Sun, *Inorg. Chem.*, 2017, **56**, 14147.

11 G. A. Senchyk, A. B. Lysenko, H. Krautscheid, E. B. Rusanov, A. N. Chernega, K. W. Kramer, S.-X. Liu, S. Decurtins, and K. V. Domasevitch, *Inorg. Chem.*, 2013, **52**, 863.

12 (*a*) C. J. Bradaric, A. Downard, C. Kennedy, A. J. Robertson and Y. Zhou, *Green Chem.*, 2003, **5**, 143; (*b*) K. J. Fraser and D. R. MacFarlane, *Aust. J. Chem.*, 2009, **62**, 309; (*c*) C. Sun, Q. Xue, Z. Hu, Z. Chen, F. Huang, H.-L. Yip and Y. Cao, *Small*, 2015, **11**, 3344.

13 (*a*) R.-B. Lin, Y. He, P. Li, H. Wang, W. Zhou and B. Chen, *Chem. Soc. Rev.*, 2019, **48**, 1362; (*b*) J. Luo, J.-W. Wang, J.-H. Zhang, S. Lai and D.-C. Zhong, *CrystEngComm*, 2018, **20**, 5884; (*c*) Y.-F. Han, Y.-X. Yuan and H.-B. Wang, *Molecules*, 2017, **22**, 266/1-266/34.

14 G. A. Jeffrey, *An Introduction to Hydrogen Bonding*, Oxford University Press, Oxford, 1997.

15 (*a*) A. Schneemann, V. Bon, I. Schwedler, I. Senkovska, S. Kaskel and R. A. Fischer, *Chem. Soc. Rev.*, 2014, **43**, 6062; (*b*) Y. Sakata, S. Furukawa, M. Kondo, K. Hirai, N. Horike, Y. Takashima, H. Uehara, N. Louvain, M. Meilikhov, T. Tsuruoka, S. Isoda, W. Kosaka, O. Sakata and S. Kitagawa, *Science*, 2013, **339**, 193; (*c*) Y.-G. Huang, Y. Shiota, M.-Y. Wu, S.-Q. Su, Z.-S. Yao, S. Kang, S. Kanegawa, G.-L. Li, S.-Q. Wu, T. Kamachi, K. Yoshizawa, K. Ariga, M.-C. Hong and O. Sato, *Nat. Comm.*, 2016, **7**, 11564.

16 (*a*) G.-P. Yang, Y.-Y. Wang, W.-H. Zhang, A.-Y. Fu, R.-T. Liu, E. K. Lermontova and Q.-Z. Shi, *CrystEngComm*, 2010, **12**, 1509; (*b*) P. Kanoo and T. K. Maji, *Eur. J. Inorg. Chem.*, 2010, **24**, 3762; (*c*) K. M. Patil, M. E. Dickinson, T. Tremlett, S. C. Moratti and L. R. Hanton, *Cryst. Growth Des.*, 2016, **16**, 1038.

17 (*a*) B. Saccoccia, A. M. Bohnsack, N. W. Waggoner, K. H. Cho, J. S. Lee, D.-Y. Hong, V. M. Lynch, J.-S. Chang and S. M. Humphrey, *Angew. Chem. Int. Ed.*, 2015, **54**, 5394; (*b*) A. E. Platero-Prats, M. Iglesias, N. Snejko, A. Monge and E. Gutierrez-Puebla, *Cryst. Growth Des.*, 2011, **11**, 1750; (*c*) H. Deng, S. Grunder, K. E. Cordova, C. Valente, H. Furukawa, M. Hmadeh, F. Gandara, A. C. Whalley, Z. Liu, S. Asahina, H. Kazumori, M. O'Keeffe, O. Terasaki, J. F. Stoddart and O. M. Yaghi, *Science*, 2012, **336**, 1018; (*d*) G. L. Maker and J. Kruger, *Int. Mater. Rev.*, 1993, **3**, 138; (*e*) L. Li, J. Gao and Y. Wang, *Surf. Coat. Tech.*, *2004*, **185**, 92.

18 (*a*) S. Choi, T. Watanabe, T.-H. Bae, D. S. Sholl and C. W. Jones, *J. Phys. Chem. Lett.*, 2012, **3**, 1136; (*b*) T.-F. Liu, L. Zou, D. Feng, Y.-P. Chen, S. Fordham, X. Wang, Y. Liu and H.-C. Zhou, *J. Am. Chem. Soc.*, 2014, **136**, 7813; (*c*) Z. Guo, G. Li, L. Zhou, S. Su, Y. Lei, S. Dang and H. Zhang, *Inorg. Chem.*, 2009, **48**, 8069.

19 (*a*) H. Furukawa, F. Gándara, Y.-B. Zhang, J. Jiang, W. L. Queen, M. R. Hudson and O. M. Yaghi, *J. Am. Chem. Soc.*, 2014, **136**, 4369; (*b*) H. Kim, S. R. Rao, E. A. Kapustin, L. Zhao, S. Yang, O. M. Yaghi and E. N. Wang, *Nat. Commun.*, 2018, **9**, 1191; (*c*) H. Kim, S. Yang, S. R. Rao, S. Narayanan, E. A. Kapustin, H. Furukawa, A. S. Umans, O. M. Yaghi and E. N. Wang, *Science*, 2017, **356**, 430; (*d*) A. Cadiau, J. S. Lee, D. D. Borges, P. Fabry, T. Devic, M. T. Wharmby, C. Martineau, D. Foucher, F. Taulelle, C.-H. Jun, Y. K. Hwang, N. Stock, M. F. De Lange, F. Kapteijn, J. Gascon, G. Maurin, J.-S. Chang and C. Serre, *Adv. Mater.*, 2015, **27**, 4775; (*e*) J. R. Álvarez, R. A. Peralta, J. Balmaseda, E. González-Zamora and I. A. Ibarra, *Inorg. Chem. Front.*, 2015, **2**, 1080.

20 (*a*) X. Zhao, B. Xiao, A. J. Fletcher, K. M. Thomas, D. Bradshaw and M. J. Rosseinsky, *Science*, 2004, **306**, 1012; (*b*) H. J. Choi, M. Dincă and J. R. Long, *J. Am. Chem. Soc.*, 2008, **130**, 7848; (*c*) R. Roque-Malherbe, *Microporous Mesoporous Mater.*, 2000, **41**, 227; (*d*) R. A. Peralta, A. Campos-Reales-Pineda, H. Pfeiffer, J. R. Alvarez, J. A. Zárate, J. Balmaseda, E. González-Zamora, A. Martínez, D. Martínez-Otero, V. Jancik and I. A. Ibarra, *Chem. Commun.*, 2016, **52**, 10273.

21 18. N. C. Burtch, H. Jasuja and K. S. Walton, *Chem. Rev.*, 2014, **114**, 10575. (b) F. Fathieh, M. J. Kalmutzki, E. A. Kapustin, P. J. Waller, J. Yang and O. M. Yaghi, *Science Advances*, 2018, **4**, eaat3198/1-eaat3198/9.

22 19. M. S. Shah, M. Tsapatsis and J. I. Siepmann, *Chem. Rev.*, 2017, **117**, 9755.

23 J. Liu, Y. Wei, P. Li, Y. Zhao and R. Zou, *J. Phys. Chem. C*, 2017, **121**, 13249.

24 (*a*) L. Hamon, C. Serre, T. Devic, T. Loiseau, F. Millange, G. Férey and G. De Weireld, *J. Am. Chem. Soc.*, 2009, **131**, 8775; (*b*) L. Hamon, H. Leclerc, A. Ghoufi, L. Oliviero, A. Travert, J.-C. Lavalley, T. Devic, C. Serre, G. Férey, G. De Weireld, A. Vimont and G. Maurin, *J. Phys. Chem. C*, 2011, **115**, 2047.

25 Y. Belmabkhout, R. S. Pillai, D. Alezi, O. Shekhah, P. M. Bhatt, Z. Chen, K. Adil, S. Vaesen, G. De Weireld, M. Pang, M. Suetin, A. J. Cairns, V. Solovyeva, A. Shkurenko, O. El Tall, G. Maurin and M. Eddaoudi, *J. Mater. Chem. A*, 2017, **5**, 3293.

26 S. Vaesen, V. Guillerm, Q. Yang, A. D. Wiersum, B. Marszalek, B. Gil, A. Vimont, M. Daturi, T. Devic, P. L. Llewellyn, C. Serre, G. Maurin and G. De Weireld, *Chem. Commun.*, 2013, **49**, 10082.

27 E. Sánchez-González, P. G. M. Mileo, M. Sagastuy-Breña, J. R. Álvarez, J. E. Reynolds III, A. Villarreal, A. Gutiérrez-Alejandre, J. Ramírez, J. Balmaseda, E. González-Zamora, G. Maurin, S. M. Humphrey and I. A. Ibarra, *J. Mater. Chem. A*, 2018, **6**, 16900.

28 (*a*) P. K. Allan, P. S. Wheatley, D. Aldous, M. I. Mohideen, C. Tang, J. A. Hriljac, I. L. Megson, K. W. Chapman, G. De

Weireld, S. Vaesen and R. E. Morris, *Dalton Trans.*, 2012, **41**, 4060; (*b*) J. A. Zárate, E. Sánchez-González, T. Jurado-Váasquez, A. Gutiérrez-Alejandre, E. González-Zamora, I. Castillo, G. Maurin, I. A. Ibarra, *Chem. Commun.*, 2019, **55**, 3049.